

Quantum conductance fluctuations and classical short-path dynamics

Hiromu Ishio* and Joachim Burgdörfer

Department of Physics, University of Tennessee, Knoxville, Tennessee 37996-1200
and Oak Ridge National Laboratory, Oak Ridge, Tennessee 37831-6377

(Received 11 August 1994; revised manuscript received 30 November 1994)

We present numerical results for ballistic-electron quantum transport through weakly open integrable circle and chaotic stadium billiards. The geometry of the pair of conducting leads is chosen in accordance with recent experiments for semiconductor microstructures [Marcus *et al.*, Phys. Rev. Lett. **69**, 506 (1992)]. The conductance as a function of the Fermi wave number displays characteristic noisy fluctuations for both the integrable and the chaotic systems. We show that structures in the conductance autocorrelation function as a function of the Fermi wave number are related to short-length classical orbits. This correspondence permits incorporation of effects of phase decoherence due to incoherent scattering into the quantum calculation.

During the last decade, remarkable advances in semiconductor fabrication technology have made it possible to produce quantum devices of submicrometer size.¹ The size of such *mesoscopic* devices is large on the atomic scale but comparable to or smaller than the phase-coherence length l_ϕ due to inelastic electron-electron (and electron-phonon) scattering at low temperatures (≈ 0.1 K). Both experimentally and theoretically, there has been considerable interest in the electronic and magnetic properties of such systems and as a result, a number of physical phenomena have been observed and predicted including universal conductance fluctuations,² weak localization,³ and Aharonov-Bohm conductance oscillations.⁴ One of the most interesting aspects is *chaotic boundary scattering* in systems formed in high-mobility GaAs/Al_xGa_{1-x}As heterostructures, where the system size is less than the elastic mean free path of electrons. In such systems, the two-dimensional motion of noninteracting electrons confined by a wall of arbitrary geometry is *ballistic*. In the ballistic regime, the shape of walls directly determines the motion of electrons colliding with them, and the classical “billiard” model successfully explains the experimental results of those systems.⁵ Nonlinear dynamics of the electrons play an important role in quantum transport through the microstructures (see, e.g., Ref. 6, and references therein).

One of the prototypes of conservative chaotic systems is the “stadium billiard.”⁷ The study of its quantum mechanics has played an important role in the identification of quantum manifestations of classical chaos.^{8,9} Studies of opened billiards pertaining to transport through mesoscopic devices have only recently begun.^{6,10-17} Major progress has been made in relating quantum conductance fluctuations with classical (non)integrable dynamics^{10,18} employing Miller’s semiclassical formulation of the S matrix.¹⁹ Generic fingerprints of regular and chaotic dynamics were identified that are related to long classical orbits and are universal (i.e., system independent). Several quantum calculations (e.g., Refs. 6, 13, and 17) were performed for a symmetric geometry for which entrance and exit leads are on opposite sides of the device facing each other. Very recently, Marcus *et al.*¹² reported experimental results of the low-temperature magnetoconductance in ballistic microstructures with the leads at an

angle of 90° relative to each other. This geometry has the advantage that it suppresses the direct transmission (i.e., transmission without collisions with the wall) and thereby enhances the sensitivity to (non)integrable dynamics inside the billiard.

In the present paper we present numerical results for classical and quantum conductance fluctuations for *weakly opened* billiards employing the same geometry as in the experiment of Marcus *et al.*¹² We focus here on the transport through the quantum dot in the absence of an external magnetic field and study conductance fluctuations as a function of the Fermi wave number. The investigation of magnetotransport properties for these systems is in progress.²⁰ We analyze the correspondence between the quantum conductance and the classical dynamics of *short orbits*. The importance of short trajectories, and hence, of nonuniversal properties of semiconductor microstructures has been highlighted in the measurement of the coherence phase-breaking length l_ϕ by Marcus *et al.*²¹ The finite value of l_ϕ implies the dominance of the short-path trajectories and the suppression of long orbits with $L > l_\phi$. Because of the imperfect experimental billiard shapes and the poorly known potential distribution inside the microstructure, only a qualitative comparison between theory and experiment is meaningful.

A stadium billiard is characterized by the radius of the semicircle a and the half-length of a straight section l . The aspect ratio $\sigma \equiv l/a$ is continuously tunable, keeping the area of the billiard $A = \pi a^2 + 4al$ fixed. For a closed stadium, the maximum Lyapunov exponent vanishes in the integrable limit ($\sigma=0$) and reaches its maximum at the fully chaotic limit ($\sigma=1$).⁷ The limit $\sigma=0$ corresponds to the circle billiard. In the following we refer to the limit $\sigma=1$ as the stadium. We use scaled lengths such that the enclosed area for both billiards is $A = \pi + 4$ (i.e., $l=a=1$ for the stadium). In the opened billiard, leads 1 and 2 are situated on the left and the lower sides of the billiard, respectively (see insets of Fig. 1) and the dc electric current passes through the leads. In the following, we call the region lying inside the billiard the “cavity region.” We choose a small lead width d with $d/\sqrt{A} = 0.0935$, which corresponds to a weakly opened billiard in which an electron entering through one lead dwells

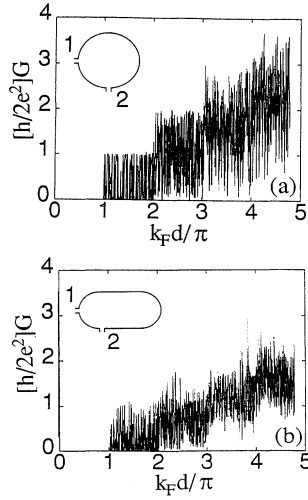


FIG. 1. Conductance G as a function of Fermi wave number k_F for (a) circle billiard; (b) stadium billiard. Insets: geometry of leads for open billiards.

inside the cavity region for a long time before exiting. Thus, chaotic and nonchaotic scattering will affect transport properties of electrons. Classically, the (non)integrability of the system manifests itself, for example, in the spectrum of dwell times inside the cavity region.^{13,18}

We determine the quantum transport properties from the solution of the time-independent Schrödinger equation using the method of Nakamura and Ishio.¹³ The wave function is subject to mixed boundary conditions: Hard-wall boundary conditions $\psi|_w=0$ are imposed for the closed segments of the boundary while the logarithmic derivative is matched across leads 1 and 2. The conductivity follows from the Landauer formula,²²

$$G = \sum_{n=1}^N G^{(n)} = \frac{2e^2}{h} \sum_{m,n=1}^N |t_{mn}|^2, \quad (1)$$

expressed in terms of the transmission amplitudes t_{mn} connecting incoming mode n in lead 1 with outgoing mode m in lead 2. Each mode corresponds to a standing wave in the lead perpendicular to the flux direction. The total number of transmitted modes is N while modes $m > N$ correspond to evanescent waves.

The conductance G displays characteristic noisy fluctuations as a function of the Fermi wave number k_F (Fig. 1). Since they are directly related to fluctuations in the S (or T) matrix [see Eq. (1)], they can be identified as Ericson fluctuations.²³ This indicates the presence of a large number of overlapping resonances (electron-scattering resonances) with a broad distribution of widths in the weakly opened billiard. Conductance fluctuations are a common feature for the circle and stadium billiards. There are, however, characteristic differences: While for the open circle billiard the conductance fluctuations $\sigma = \langle \delta G^2 \rangle^{1/2}$ increase with k_F from $\sigma \approx 0.37$ (in units of $2e^2/h$) for $N=1$ to $\sigma = 0.63$ for $N=4$, they are, for the open-stadium billiard, of the order $\sigma = 0.33$ independent of k_F . Furthermore, the average con-

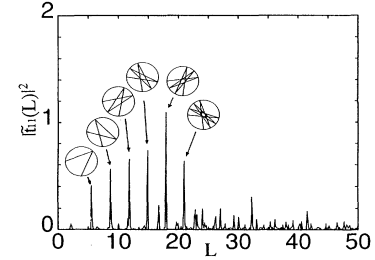


FIG. 2. Fourier transform of transmission amplitude $t_{11}(k_F)$ and corresponding classical paths for the open-circle billiard. The scaled length L corresponds to a fixed area of the cavity region $A = \pi + 4$.

ductance is smaller for the open stadium than for the circle billiard. These features can be understood in terms of universal conductance fluctuations² and weak localization,³ found in diffusive disordered systems, and have also been observed in other geometries.⁶

In the following we explore the classical quantum correspondence for conduction fluctuations in more detail. To this end we have calculated the Fourier transform of the transmission amplitude $t_{11}(k_F)$ (Fig. 2). Note that in the experiment¹² several modes contribute. According to semiclassical theory,^{10,19}

$$t_{mn} \approx \sum_s \sqrt{D_{mn}^s} \exp\left(\frac{i}{\hbar} \int_s \mathbf{p} \cdot d\mathbf{x} - i\pi \frac{\alpha_s}{2}\right), \quad (2)$$

where α_s is the Maslov index, the amplitude factor $D_{m,n}^s$ measures the spread of classical trajectories near the paths, and a sum is taken over all classical trajectories s connecting incoming channel n and outgoing channel m . The length-dependent phase factor reduces for the billiard to $\exp(ik_F \cdot L_s)$, where L_s is the length of the trajectory s extending from the entrance to the exit lead. In the semiclassical limit, the Fourier transform of $t_{m,n}$, $\tilde{t}_{mn}(L)$, is therefore expected to display peaks at values of L corresponding to paths connecting the two leads. In case of the open-circle billiard, the power spectrum $|\tilde{t}_{11}(L)|^2$ exhibits a sequence of prominent peaks in the short-length region ($L \lesssim 21$), which correspond exactly to a sequence of classical “asterisk” paths connecting the entrance and exit in the cavity (Fig. 2). Other modes give similar peak structures, however, with different peak strengths. On the other hand, there appears to be no comparably sharp peak structure for the open-stadium billiard (not shown). The difference may be understood in terms of the underlying classical dynamics. In the circular billiard, different bundles of trajectories connecting the two leads are separated from each other, each of which has a finite measure characteristic of integrable systems. In turn, each bundle is associated with a peak in $|\tilde{t}_{11}(L)|^2$. On the other hand, the absence of sharp peaks in $|\tilde{t}_{11}(L)|^2$ for the stadium billiard reflects the fact that trajectories connecting the two leads are more uniformly spread out over the length spectrum, as discussed below in more detail. Furthermore, we have observed that bundles of trajectories with small angles of incidence display a propensity for influencing the quantum t matrix elements while trajectories other than the asterisk trajectories with larger angles of incidence are suppressed.

Quantum conductance fluctuations can be characterized by the wave-number-dependent autocorrelation function

$$\Gamma(\kappa) = \langle \delta G(k_F - \kappa/2) \delta G(k_F + \kappa/2) \rangle_{k_F}, \quad (3)$$

where $\delta G \equiv G - \langle G \rangle_{k_F}$. The average $\langle \rangle_{k_F}$ is taken over $1.190 \leq k_F d / \pi \leq 4.584$. This average corresponds in the experiment to an average over the gate voltage or a thermal average. The Fourier transform of the autocorrelation function

$$C_{qm}(L) = \frac{2}{\pi} \Gamma(0)^{-1} \int_0^\infty d\kappa \Gamma(\kappa) \cos(\kappa L) \quad (4)$$

corresponds in the semiclassical limit⁶ to the normalized classical path-length correlation function

$$C_{qm}(L) \approx C_{cl}(L) = \int_0^\infty dL' P_{cl}(L'+L) P_{cl}(L') \times \left(\int_0^\infty dL' P_{cl}(L')^2 \right)^{-1}, \quad (5)$$

where the classical path-length spectrum $P_{cl}(L)$ is given by a Monte Carlo sampling of trajectories entering through lead 1 with uniform density across the lead. Based on simple classical arguments employing the ergodicity of the trajectories for a weakly opened billiard whose closed counterpart is chaotic, the path-length distribution should be universal and should be exponentially decaying,^{11,18}

$$P_0(L) = \gamma e^{-\gamma L}, \quad (6)$$

with $\gamma = 2d/A\pi$. Equation (6) has been verified numerically in the limit of long orbits.^{6,14} By inverse Fourier transform, the exponential path-length distribution gives a Lorentzian conductance autocorrelation function

$$\Gamma_0(\kappa)/\Gamma_0(0) = 1/[1 + (\kappa/\gamma)^2]. \quad (7)$$

Our analysis of the conductance fluctuations in the stadium shows that Eq. (6) is not yet valid in the region of path length $L \lesssim l_\phi$ accessible in the experiment. From the measured phase-breaking rate in GaAs/Al_xGa_{1-x}As ballistic quantum dots²¹ at low temperatures, one can estimate $l_\phi \approx 87$ in our scaled units. Elastic small-angle scattering, also present in the experiment, does not break the quantum coherence. Figure 3 shows our Monte Carlo simulation of the classical path-length distribution for the stadium billiard pertaining to the geometry of Ref. 12. Within the region $L \lesssim l_\phi$, the path-length distribution is a highly structured function displaying, in addition to the direct path connecting the entrance with the exit lead, a sequence of almost equidistant broad peaks in the short-length region $L \lesssim 70$. The period of these peaks corresponds approximately to the perimeter length of the cavity region (whispering gallery trajectories). For longer path lengths the proliferation of orbits tends to average out this structure resulting in a coarse-grained exponential distribution with a decay constant $\gamma = 0.0223$ predicted by Eq. (6) (dotted line in Fig. 3).

The structures in the classical short-length spectrum are directly related to the conductance autocorrelation function

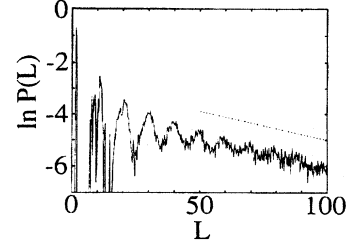


FIG. 3. Classical path-length spectrum $P_{cl}(L)$ for the stadium billiard. Dotted line represents exponential decay with exponent $\gamma = 0.0223$ predicted by Jensen (Ref. 11). The scaled length L corresponds to a fixed area of the cavity region $A = \pi + 4$.

(Fig. 4). $\Gamma(\kappa)$ clearly deviates from a simple Lorentzian form predicted by Eq. (7). Similar deviations have been observed previously for the magnetoconductances in a different geometry.⁶ The prominent peak at $\kappa d/\pi \approx 0.05$ is directly related to the oscillations in $P_{cl}(L)$. The point to be emphasized is that the strong deviation of $\Gamma(\kappa)$ from a Lorentzian shape is not due to the breakdown of the semiclassical approximation itself (even at the comparably low mode numbers studied here and in the experiment), but is due to the exponential approximation to the exact classical path-length distribution.

Accordingly, inverse Fourier transform of the exact classical path-length correlation function $C_{cl}(L)$ reproduces the quantum autocorrelation function quite well (Fig. 4). In the limit of very small κ corresponding to large L (inset of Fig. 4), the Lorentzian approximation becomes valid as expected from the convergence of the exact path-length distribution to an exponential for large L . This limit is, however, not yet accessible in the experiment since it exceeds the quantum coherence length beyond which the description of the billiard as a nondissipative and phase-coherent quantum system breaks down.

The incorporation of phase breaking due to incoherent scattering processes within the description of a Hamiltonian quantum system is *a priori* not obvious. However, the close classical quantum correspondence observed for the conduc-

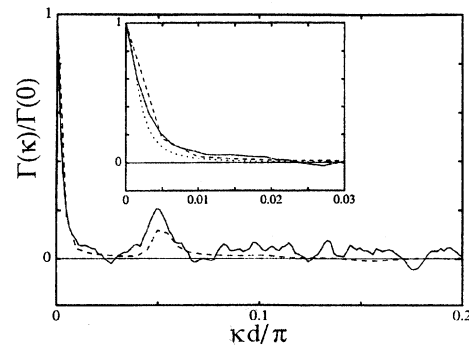


FIG. 4. Conductance autocorrelation function $\Gamma(\kappa)$ (solid lines) and Fourier transform of $C_{cl}(L)$ for the stadium billiard averaged over intervals $\Delta L = \pm 2$ (dashed line). Inset: Partial magnification for $\kappa d/\pi \leq 0.03$. Dotted curve represents the Fourier transform of $C_{cl}(L)$ using $P_0 \propto \exp(-\gamma L)$, i.e., a Lorentzian $1/[1 + (\kappa/\gamma)^2]$.

tance fluctuation autocorrelation function lends itself to a simple approximate prescription that exploits the fact that on the classical level incoherent loss can be easily incorporated treating the phase-breaking length l_ϕ as an effective mean free path from phase-breaking inelastic collisions.²¹ Phase-breaking scattering events lead to an exponential decay of contributing trajectories, $\sim e^{-L/l_\phi}$. The path-length distribution can now be corrected for by taking into account the incoherent loss,

$$P^\phi(L) = P(L)e^{-L/l_\phi}. \quad (8)$$

Since for large L , $P(L)$ converges to the universal distribution $P_0(L)$, we can approximate $C_{qm}^\phi(L) \approx e^{-L/l_\phi} C_{qm}(L)$. Inverse Fourier transform yields the modified quantum autocorrelation function

$$\Gamma_\phi(\kappa)/\Gamma_\phi(0) \approx \int_0^\infty dL \cos(L\kappa) C_{qm}(L) e^{-L/l_\phi}, \quad (9)$$

which takes into account incoherent scattering, i.e., long trajectories beyond the phase-breaking length are exponentially suppressed. Figure 5 illustrates the resulting correction of the autocorrelation function for conductance fluctuations due to finite l_ϕ . The peak at $\kappa d/\pi \approx 0.05$ is still present but the negative “overshoot” in the conductance correlation function disappears. Structures in $\Gamma(\kappa)$ are obviously sensitive to the value of the coherence length. This dependence may offer the opportunity of an independent determination of the phase-breaking length in mesoscopic devices.

In conclusion, we have shown that conductance fluctuations in the weakly open quantum billiard carry clear signa-

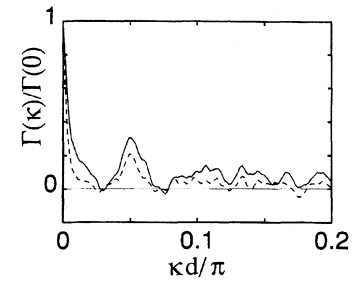


FIG. 5. Comparison between the conductance fluctuation autocorrelations $\Gamma(\kappa)$ [Eq. (3), dashed line] and $\Gamma_\phi(\kappa)$ [Eq. (8), solid line] taking into account the coherence phase-breaking length $l_\phi \approx 87$.

tures of the classical orbits with short path length. They are expected to be observable in GaAs/Al_xGa_{1-x}As ballistic quantum dots²¹ since the relevant path lengths are shorter than the phase-coherence length in these semiconductor heterostructures. The remarkably close classical quantum correspondence suggests a simple approximate recipe for taking phase breaking into account by Fourier transform of the modified path-length spectrum in which long orbits exceeding the phase coherence length are exponentially suppressed.

This work was supported in part by the National Science Foundation and by the U.S. Department of Energy, Office of Basic Energy Sciences, Division of Chemical Sciences, under Contract No. DE-AC05-84OR21400 with Martin Marietta Energy Systems, Inc.

*Present and permanent address: Department of Physics, Kyoto University, Kyoto 606, Japan.

¹See, e.g., *Nanostructure Physics and Fabrication*, edited by M. A. Reed and W. P. Kirk (Academic, New York, 1989).

²P. A. Lee and A. D. Stone, Phys. Rev. Lett. **55**, 1622 (1985); B. L. Altshuler, Pis'ma Zh. Eksp. Teor. Fiz. **41**, 530 (1985) [JETP Lett. **41**, 648 (1985)]; P. A. Lee, A. D. Stone, and H. Fukuyama, Phys. Rev. B **35**, 1039 (1987).

³For a review, see, e.g., G. Bergmann, Phys. Rep. **107**, 1 (1984).

⁴S. Washburn and R. A. Webb, Adv. Phys. **35**, 375 (1986).

⁵M. L. Roukes, A. Scherer, and B. P. Van der Gaag, Phys. Rev. Lett. **64**, 1154 (1990); M. L. Roukes and O. L. Alerhand, *ibid.* **65**, 1651 (1990); C. W. J. Beenakker and H. van Houten, in *Electronic Properties of Multilayers and Low-Dimensional Semiconductor Structures*, edited by J. M. Chamberlain, L. Eaves, and J.-C. Portal (Plenum, New York, 1990); in *Solid State Physics*, edited by H. Ehrenreich and D. Turnbull (Academic, New York, 1991), Vol. 44, p. 1.

⁶H. U. Baranger, R. A. Jalabert, and A. D. Stone, Chaos **3**, 665 (1993).

⁷L. A. Bunimovich, Funct. Anal. Appl. **8**, 254 (1974); G. Benettin and J. M. Strelcyn, Phys. Rev. A **17**, 773 (1978).

⁸See, e.g., M. C. Gutzwiller, *Chaos in Classical and Quantum*

Mechanics (Springer, New York, 1990).

⁹E. J. Heller, Phys. Rev. Lett. **53**, 1515 (1984).

¹⁰R. A. Jalabert, H. U. Baranger, and A. D. Stone, Phys. Rev. Lett. **65**, 2442 (1990).

¹¹R. V. Jensen, Chaos **1**, 101 (1991).

¹²C. M. Marcus, A. J. Rimberg, R. M. Westervelt, P. F. Hopkins, and A. C. Gossard, Phys. Rev. Lett. **69**, 506 (1992).

¹³K. Nakamura and H. Ishio, J. Phys. Soc. Jpn. **61**, 3939 (1992).

¹⁴W. A. Lin, J. B. Delos, and R. V. Jensen, Chaos **3**, 655 (1993).

¹⁵M. J. Berry, J. A. Katine, C. M. Marcus, R. M. Westervelt, and A. C. Gossard, Surf. Sci. **305**, 495 (1994).

¹⁶M. W. Keller, O. Millo, A. Mittal, D. E. Prober, and R. N. Sacks, Surf. Sci. **305**, 501 (1994).

¹⁷K. Nakamura, K. Ito, and Y. Takane, J. Phys. A (to be published).

¹⁸R. Blümel and U. Smilansky, Phys. Rev. Lett. **60**, 477 (1988).

¹⁹W. H. Miller, Adv. Chem. Phys. **25**, 69 (1974).

²⁰X. Yang, H. Ishio, and J. Burgdörfer (unpublished).

²¹C. M. Marcus, R. M. Westervelt, P. F. Hopkins, and A. C. Gossard, Phys. Rev. B **48**, 2460 (1993).

²²R. Landauer, IBM J. Res. Dev. **1**, 223 (1957).

²³T. Ericson and T. Mayer-Kuckuk, Annu. Rev. Nucl. Sci. **16**, 183 (1966).